THE IMPACT OF DIFFERENT BASE NANOFLUIDS ON THE FLUID FLOW AND HEAT TRANSFER CHARACTERISTICS IN RHOMBUS MICROCHANNELS HEAT SINK

Altayyeb ALFARYJAT[1], Adina-Teodora GHEORGHIAN[2], Ahmed NABBAT[3], Mariana-Florentina ȘTEFĂNESCU[4], Alexandru DOBROVICESCU[5]

The heat transfer and laminar flow characteristics of the 3D rhombus microchannels heat sink (RMCHS) using nanoparticles of Al_2O_3 mixed with different base fluids are numerically investigated. In this study, four base fluids are examined, such as: pure water, engine oil, glycerin and ethylene glycol with Al_2O_3 concentration of 4% and nanoparticles diameter of 25 nm. The heat flux was fixed at 500 kW/m^2 and the inlet velocity temperature was set at 290 K. It is concluded that Al_2O_3-water has the lowest temperature, highest heat transfer characteristics and lowest thermal resistance compared to the other base fluids. Moreover, the friction factor for all base fluids studied showed no significant differences.

Keywords: microchannels heat sink, nanofluids, CFD modelling, rhombus microchannels, base fluids.

1. Introduction

Over the past decades, microchannels heat sink (MCHS) has become one of the most important methods of removing heat generated in electronic chips, photovoltaic cells and nuclear components, pumps, biomedical and biochemical analysis instruments. To enhance the heat transfer, nanofluids (colloidal suspensions of nanoparticles made of metals, oxides, carbides, or carbon nanotubes in water, ethylene glycol or engine oil) are considered as working fluids instead of pure water.

Najafabadi and Moraveji [1], Anbumeenakshi and Thansekhar [2] investigated numerically and experimentally the heat transfer characteristics and

[1] PhD student, Dept. of Eng. Thermodynamics, Engines, Thermal and Refrigeration Equipment, University POLITEHNICA of Bucharest, Romania, e-mail: altayyeb81@yahoo.com
[2] Assist Prof., Dept. of Eng. Thermodynamics, Engines, Thermal and Refrigeration Equipment, University POLITEHNICA of Bucharest, Romania, e-mail: adina_gheorghian@yahoo.com
[3] Master, Dept. of Eng. Thermodynamics, Engines, Thermal and Refrigeration Equipment, University POLITEHNICA of Bucharest, Romania, e-mail: ahmedalageely@gmail.com
[4] Prof., Dept. of Equipment and industrial processes, University POLITEHNICA of Bucharest, Romania, e-mail: marianastefanescu2007@yahoo.com
[5] Prof., Dept. of Eng Thermodynamics, Engines, Thermal and Refrigeration Equipment, University POLITEHNICA of Bucharest, Romania, e-mail: adobrovicescu@yahoo.com

fluid flow through a rectangular MCHS using alumina-water nanofluid as a base fluid. The results showed that increasing the Reynolds number and volume fraction of nanoparticles led to improved convective heat transfer coefficient and decrease the maximum temperate. Moreover, the thermal resistance decreases with the increase of Reynolds number and volume fraction of nanoparticles.

Kumar and Kumar [3] examined experimentally the Al_2O_3, TiO_2, MgO and ZnO nanoparticles mixed with water and ethylene glycol (EG) in MCHS. The results showed that Al_2O_3-water had better heat transfer characteristics than other nanofluids. Abdollahi et al. [4] examined SiO_2, Al_2O_3, ZnO and CuO nanoparticles dispersed in pure water in rectangular MCHS with V-typed. It is noticed that the SiO_2 nanofluid with nanoparticles diameter of 30 nm had the best performance among other tested nanofluids.

Uysal et al. [5] investigated the effect of ZnO-Ethylene glycol (EG) nanofluid through rectangular MCHS. The authors concluded that the temperature and the pressure increase when the nanoparticle volume fraction increases. Agnihotri and Sharma [6] found out that heat transfer coefficient doubles in comparison to the water as a coolant in trapezoidal MCHS by using TiO_2-water as a based fluid.

Sivakumar et al. [7] reported experimentally that CuO-H_2O nanofluids have better heat transfer in the MCHS than Al_2O_3-H_2O nanofluid. Mashaeil et al. [8] found that pressure drop occurs at highest nanoparticle volume fraction (φ=8%) and Reynolds number (Re=100).

The aim of this paper is to investigate the fluid flow and heat transfer characteristics of alumina nanoparticles with four different base-fluids (pure water, glycerin, ethylene glycol, and engine oil) in a rhombus MCHS with a constant wall heat flux. Predictions are validated with referenced experimental data of Ho et al. [9]. Various parameters, such as: heat sink top wall temperature, heat transfer coefficient, friction factor, thermal resistance and pumping power are studied in order to evaluate the performance of rhombus MCHS.

2. MCHS model

2.1. Model description

In this paper, a rhombus microchannels heat sink with nanofluids was analyzed. By using 26 microchannels for fluid flow through the heat sink, the heat supplied by the top plate of MCHS was removed. The specified dimensions of rhombus shape MCHS are given in Table 1. Fig. 1 (a, b) shows the schematic diagrams of the geometrical shape of the microchannels heat sink.

Table 1

Dimensions of rhombus MCHS

W_{hs}(μm)	L_{hs}(μm)	H_{hs}(μm)	P_{ch}(μm)	Q_{ch}(μm)	X_{ch}(μm)	Φ_1	Φ_2	S(μm)	D_h(μm)
22000	10000	1500	200	340	200	60	120	447	170

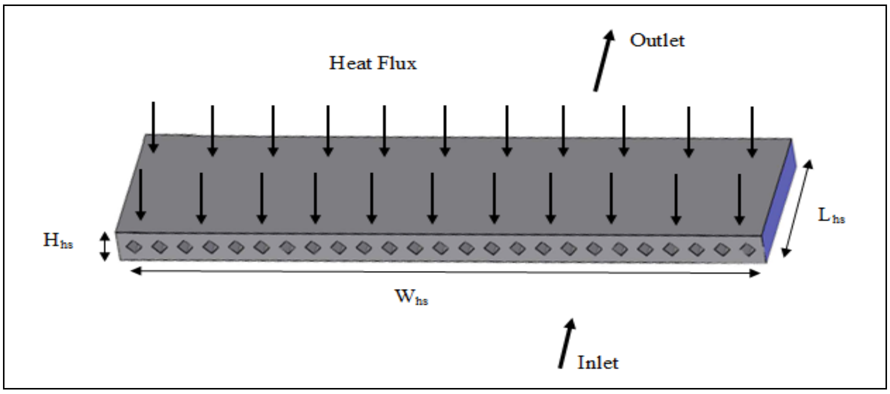

(a)

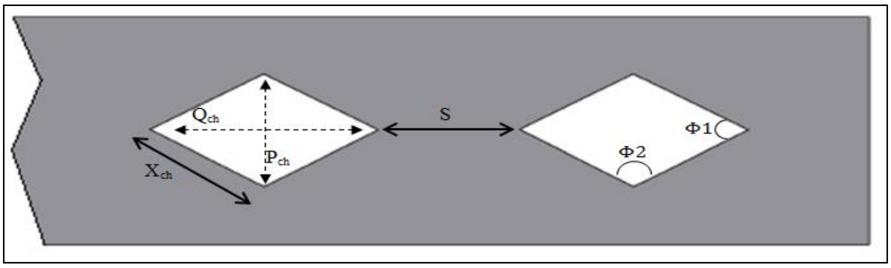

(b)

Fig. 1: (a) Schematic diagram of the computational domain; (b) cross section rhombus cross-section shaped MCHS

where W_{hs} is the heat sink width, L_{hs} is the heat sink length, H_{hs} is the heat sink high, P_{ch} is the channel height, Q_{ch} is channel width, X_{ch} is the side of the channel, S is the distance between two microchannels, $\phi 1, \phi 2$ are the channel's angles.

2.2 Governing Equations

In completing the CFD analysis for the rhombus MCHS, it is required to build up the governing equations (momentum, continuity and energy). For the exact case of heat flux's effect, the fluid flow through rhombus microchannels, the following assumptions were made to solve the governing equations: (1) steady-state and 3D heat transfer and fluid flow, (2) the fluid flow is laminar, incompressible and single phase, (3) the temperature-independent is the physical property of the fluid flow and heat sink material, (4) all the surrounding surfaces of MCHS are adiabatic, except for the microchannel top plate, for which the heat flux is included in the study and it is produced by electronic chips.

Based on the above assumptions, the energy, momentum and continuity equations for this study can be written as [10]:

The continuity equation:

$$\frac{\partial U}{\partial X}+\frac{\partial V}{\partial Y}+\frac{\partial W}{\partial Z}=0 \tag{1}$$

The X-Momentum equation:

$$U\frac{\partial U}{\partial X}+V\frac{\partial U}{\partial Y}+W\frac{\partial U}{\partial Z}=-\frac{d\hat{p}}{dX}+\frac{1}{\mathrm{Re}}\left(\frac{\partial^2 U}{\partial X^2}+\frac{\partial^2 U}{\partial Y^2}+\frac{\partial^2 U}{\partial Z^2}\right), \tag{2}$$

The Y-Momentum equation:

$$U\frac{\partial V}{\partial X}+V\frac{\partial V}{\partial Y}+W\frac{\partial V}{\partial Z}=-\frac{d\hat{p}}{dY}+\frac{1}{\mathrm{Re}}\left(\frac{\partial^2 V}{\partial X^2}+\frac{\partial^2 V}{\partial Y^2}+\frac{\partial^2 V}{\partial Z^2}\right), \tag{3}$$

The Z-Momentum equation:

$$U\frac{\partial W}{\partial X}+V\frac{\partial W}{\partial Y}+W\frac{\partial W}{\partial Z}=-\frac{d\hat{p}}{dZ}+\frac{1}{\mathrm{Re}}\left(\frac{\partial^2 U}{\partial X^2}+\frac{\partial^2 U}{\partial Y^2}+\frac{\partial^2 U}{\partial Z^2}\right), \tag{4}$$

The energy equation:

$$U\frac{\partial \theta}{\partial X}+V\frac{\partial \theta}{\partial Y}+W\frac{\partial \theta}{\partial Z}=\frac{1}{\mathrm{Re}\,.\,\mathrm{Pr}}\left(\frac{\partial^2 \theta}{\partial X^2}+\frac{\partial^2 \theta}{\partial Y^2}+\frac{\partial^2 \theta}{\partial Z^2}\right), \tag{5}$$

where *U,V,W* are the dimensionless velocity in x, y, z coordinates and *X, Y, Z* are the dimensionless Cartesian coordinates.

The fluid temperature profile and pressure drops along the MCHS are solved by employing these governing equations with defined boundary conditions and the obtained data are then used to examine the fluid flow and thermal performances of the fluids along the MCHS. Another assumption made is that the channel heat sink entrance is at Z=0. Two important boundary conditions can be defined from the current fluid flow through the microchannel heat sink and also the top surface heat removal of the heat sink. The temperature of the inlet water is 290 K and the inlet water velocity of the microchannel depends on Reynolds number. In this paper, the Reynold's number is fixed at 700, whereas the top plate heat flux of the heat sink is set at 500 kW/m^2. The inlet velocity (u_{in}) is calculated as:

$$u_{in}=\frac{\mathrm{Re}\,\mu}{\rho D_h}, \tag{6}$$

where *Re* is the Reynolds number, μ is the viscosity of the fluid, ρ is the density of the fluid, D_h is the hydraulic diameter of the channel. The solid thermal conductivity is computed as $k_s = 202.4 W/m.K$.

2.3. Numerical procedures

The numerical calculations were done by solving the governing conservation equation - eqs. (1) – (5) - using the finite volume method (FVM) along with the boundary conditions [11]. The flow field of the MCHS was solved by using the SIMPLEC algorithm [12]. Using GAMBIT software, the geometry of CFD regions was created and the mesh was generated. By using the CFD technique, the effects of geometrical parameters on MCHS were investigated by using nanofluids as working fluids instead of water base fluids. The second-order upwind differencing scheme is considered for the convective terms. To find out the velocity components, the momentum equation is solved. The continuity equation is used to update the pressure value.

2.4 Code Validation

An experimental study carried out by Ho et al. [9] was used in order to validate the current results. However, their experimental research was mainly focused on the performance of rectangular cross-sectional MCHS. Al_2O_3 - water was used as a working fluid for a 25-channels heat sink with Reynolds number ranging between 100 and 1000. One may observe that the present code results are close to the previous experimental published results, as shown in Fig. 2.

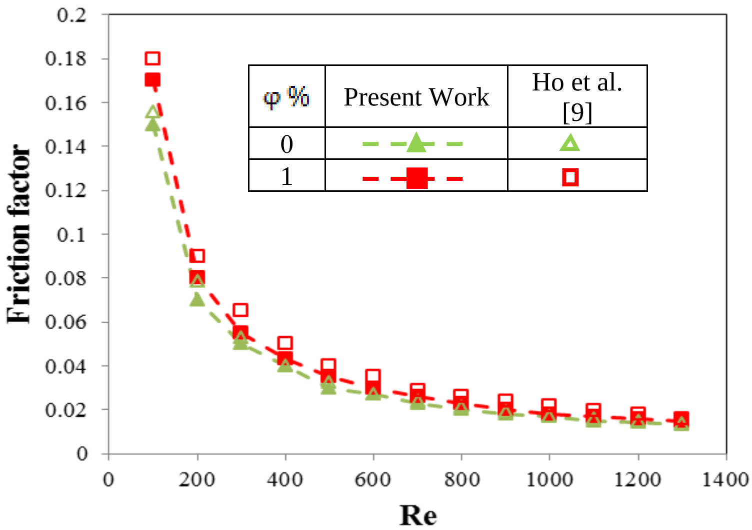

Fig. 2. Variation of the friction factor versus Reynolds number for different volume fractions of Al_2O_3-H_2O

2.5. Grid Independence Test

The grid independence test of hexahedral cells in all cross-section MCHS is determined by a series of tests with different numbers of cells in order to obtain the most suitable mesh for the current geometry. Fig. 3 presents the mesh cells of the rhombus cross-section MCHS at q_w=500 kW/m^2.

Three mesh cells were used: 2×10^5, 6×10^5 and 9×10^5 grids. The results obtained are displayed in Fig. 3. This figure represents the top wall temperature across the microchannels heat sink versus Reynolds number. It can be noticed that the results of the 6×10^5 and 9×10^5 grids for top wall temperature are almost at an equal grid. A computational cell with 6×10^5 grid is employed for all the numerical results in order to lowering the time needed to calculate the results compared to 9×10^5 grids.

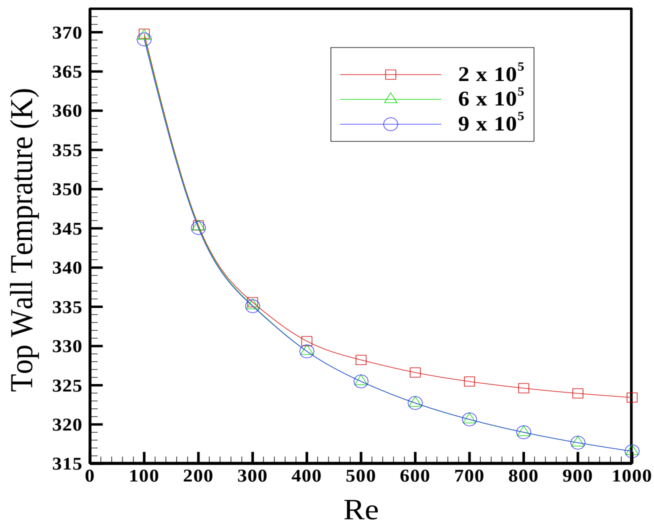

Fig. 3. Top wall temperature versus different Reynolds numbers for rhombus MCHS (D_h = 170 µm) using three different grids

2.6. Nanofluid Thermal properties

Fundamentally, the properties required for the simulations are: effective specific heat (C_{peff}), effective thermal conductivity (K_{eff}), effective mass density (ρ_{eff}), and effective dynamic viscosity (μ_{eff}). The main physical properties of interest are: specific heat, density, viscosity and thermal conductivity, which have been analyzed based on the mixing theory. The thermophysical properties of nanoparticles Al_2O_3, all types of base fluids, and nanofluids are shown in Table 2.

The density of nanofluids can be obtained from the following equation, as stated by [13]:

$$\rho_{nf} = (1-\phi)\rho_{bf} + \phi\rho_{np}, \tag{7}$$

where ρ_{nf} is the mass density of the based fluid, ρ_{np} is the mass density of the solid nanoparticles, $\emptyset$ is the particle volume fraction.

The effective heat capacity of the nanofluids at constant pressure drops of nanofluids, $(\rho\ C_p)_{nf}$ can be determined using the following equation, according to [13]:

$$\left(\rho c_p\right)_{nf} = (1-\phi)\left(\rho c_p\right)_{bf} + \phi\left(\rho c_p\right)_{np}, \quad (8)$$

where $C_{p.f}$ is the heat capacity of the base fluid, $C_{p.np}$ is the heat capacity of solid nanoparticles.

By using Brownian motion of nanoparticles in MCHS, the thermal conductivity may be found according to [14]:

$$k_{eff} = k_{Static} + k_{Brownian} \quad (9)$$

Static thermal conductivity:

$$k_{Static} = k_{bf}\left[\frac{k_{np}+2k_{bf}-2\left(k_{bf}-k_{np}\right)\phi}{k_{np}+2k_{bf}+\left(k_{bf}-k_{np}\right)\phi}\right] \quad (10)$$

Brownian thermal conductivity:

$$k_{Brownian} = 5\times10^4 \beta\phi\rho_{bf}c_{p,bf}\sqrt{\frac{kT}{2\rho_{np}R_{np}}}\cdot f(T,\phi), \quad (11)$$

where the Boltzmann's constant is $k = 1.3807\times10^{-23}\ J/K$.

Based on Vajjha and Da [15], the modeling function β of (Al_2O_3) is:

$$\beta = 8.4407(100\phi)^{-1.07304}\ . \quad (12)$$

Also, the modeling function $f\,(T, \emptyset)$ is:

$$f(T,\phi)=\left(2.8217\times10^{-2}\phi+3.917\times10^{-3}\right)\left(\frac{T}{T_\circ}\right)+\left(-3.0699\times10^{-2}\phi-3.91123\times10^{-3}\right) \quad (13)$$

The effective viscosity equation of the nanofluids can be calculated, based on Corcione [16], as:

$$\frac{\mu_{eff}}{\mu_{bf}} = \frac{1}{1-34.87\left(d_{np}/d_{bf}\right)^{-0.3}\phi^{1.03}} \quad (14)$$

The equivalent diameter of the base fluid molecule is calculated as:

$$d_{bf} = \left[\frac{6M}{N\pi\rho_{bf}}\right]^{1/3}, \quad (15)$$

where N is the Avogadro number = 6.022 x10^{23} mol^{-1}, M is the molecular weight of base fluid, nf is the nanofluid, b_f is the base fluid, np represents the nanoparticles used.

Table 2

Thermophysical properties of the nanoparticles, base fluids and nanofluids.

Properties	Nanoparticle (Al_2O_3)	Base fluid (water)	Nanofluid H_2O–Al_2O_3 , 4%, np=25 nm
ρ (kg/m^3)	3970	998.2	1117.648
μ (N.s/m^3)	-	0.001003	0.0013462
C_p (J/kg. K)	765	4182	3812.3821
K (W/m.K)	40	0.6	0.6592267
Properties	Nanoparticle (Al_2O_3)	Ethylene Glycol [17]	EG–Al_2O_3, 4%, np=25 nm
ρ (kg/m^3)	3970	1118.8	1232.848
μ (N.s/m^3)	-	0.0247	0.0415338
C_p (J/kg. K)	765	2368	2161.52167
K (W/m.K)	40	0.248	0.29246043
Properties	Nanoparticle (Al_2O_3)	Engine Oil [17]	EO –Al_2O_3 ,4%, np=25 nm
ρ (kg/m^3)	3970	890	1013.2
μ (N.s/m^3)	-	0.99	1.77039058
C_p (J/kg. K)	765	1868	1695.12554
K (W/m.K)	40	0.145	0.17174005
Properties	Nanoparticle (Al_2O_3)	Glycerin [17]	Gly-Al_2O_3,4%,np=25 nm
ρ (kg/m^3)	3970	1265.8	1373.968
μ (N.s/m^3)	-	1.85	3.17026292
C_p (J/kg. K)	765	2367	2181.8446
K (W/m.K)	40	0.286	0.33685617

3. Results and discussion

The influence of rhombus shape on the MCHS thermal and hydrodynamic performance using different base fluids with Al_2O_3 as a working fluid at D_h=170 µm was analyzed. The Reynolds number was fixed at 700 for all channels flow shapes. The heat flux on top wall of MCHS was set at 500 kW/m^2.

In this section, the liquid flow and the heat transfer characteristics in rhombus cross-section MCHS using various types of conventional base fluids such as: engine oil, ethylene glycol ($C_2H_4(OH)_2$), glycerin ($C_3H_5(OH)_3$), and pure water are investigated. The reason of using different types of base fluids was to investigate if there is any enhancement in the cooling performance of the MCHS.

For all types of base fluids, Al_2O_3 nanoparticles with particle volume fraction equal to 4% and nanoparticle diameter (*dp*) of 25nm were considered. Regarding the thermos-physical properties of the base fluids, engine oil-Al_2O_3, EG-Al_2O_3 and glycerin-Al_2O_3 have higher viscosity than water-Al_2O_3, while the thermal conductivity for basic fluids is lower than that of water-Al_2O_3.

This paper is focused on studying the top wall temperature, heat transfer coefficient, friction factor, thermal resistance and pumping power.

3.1. Top Wall Temperature

The effects of different types for variation of the temperature along the top wall of MCHS at Re =700 are presented in Figs. 4 and 5. It can be noticed that the heat sink top wall using water–Al_2O_3 has the lowest temperature among all types of base fluids, while engine oil-Al_2O_3, ethylene glycol (EG)-Al_2O_3 and glycerin-Al_2O_3 have the highest temperature top wall. This phenomenon can be justified by the fact that Al_2O_3-H_2O has higher thermal conductivity than the rest of base fluids, which is consistent with the finding of Ahmed et al. [18] (see Table 2). Thus, it is reasonable to expect that the addition of aluminum nanoparticles in water would lead to an enhancement of the heat transfer coefficient compared to other base fluids. Moreover, the temperature along the top wall length increases for all types of base fluids and pure water due to the fact that the heat flux along the heat sink is carried by the fluid. Fig. 4 shows the top wall contours while using pure water with Al_2O_3.

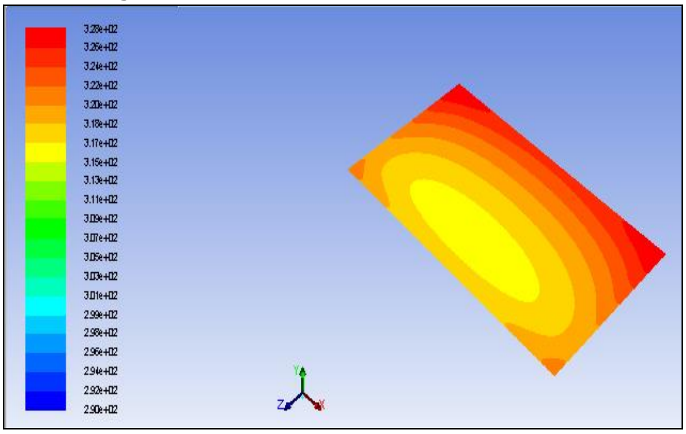

Fig. 4. Top wall contours

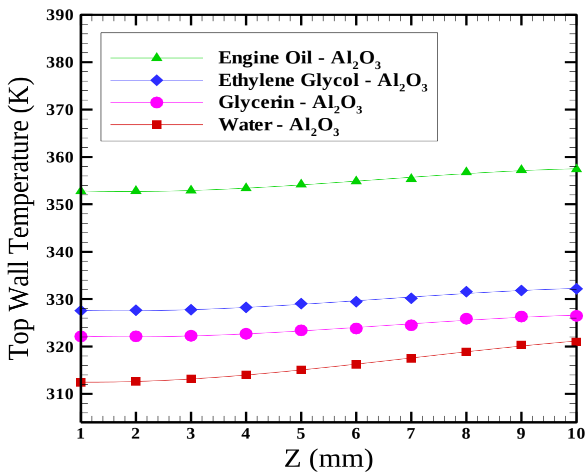

Fig. 5. Temperature along the length of top wall of MCHS for all base fluids

3.2. Heat Transfer Coefficient

The heat transfer coefficient for each microchannel of the rhombus cross-section MCHS using various base fluids at Re=700 is presented in Fig. 6. The results show that Al_2O_3-H_2O has the highest heat transfer coefficient, while glycerin-Al_2O_3, ethylene glycol-Al_2O_3, and engine oil-Al_2O_3 have lower values heat transfer. This phenomenon can be justified by the fact that water-Al_2O_3 has high thermal conductivity, which shows better heat transfer performance than other base fluids, according to Wang et al. [19].

The channels 13 and 14 have the highest heat transfer coefficients, as shown in Fig. 6. For the rest of channels, heat transfer coefficient values decrease depending on their distance from the wall.

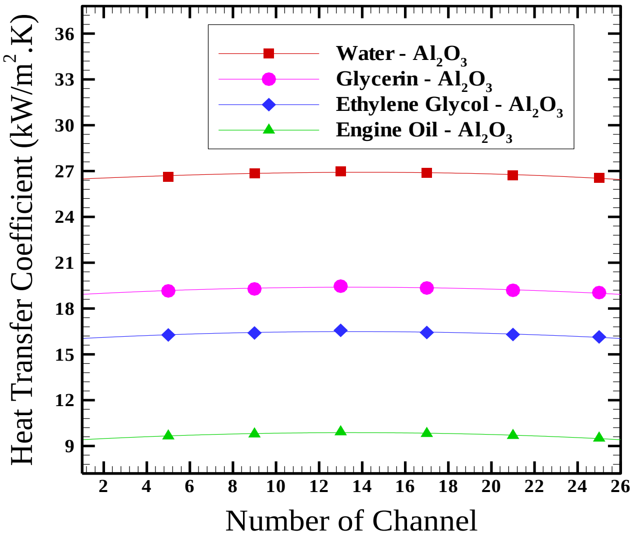

Fig. 6. Heat transfer coefficient versus number of channel for pure water and several of base fluids

3.4. Friction Factor

Laminar flow becomes an important issue particularly when passing through rough channels. The friction factor for fluids can be calculated using the Darcy equation [20]:

$$f = \frac{2.D_h.\Delta p}{\rho.u_{in}^2.L_{ch}}, \tag{16}$$

The impact of using various base fluids on the friction factor along with the length of the channel number 14 for rhombus cross-section MCHS at Re=700 and q_w = 500 kW/m^2 is presented in Fig. 7. The obtained results show that the trend of friction factor for all types of base fluids is identical and it decreases along the length of channel. For the friction factor there was no significant difference between all types of examined base fluids.

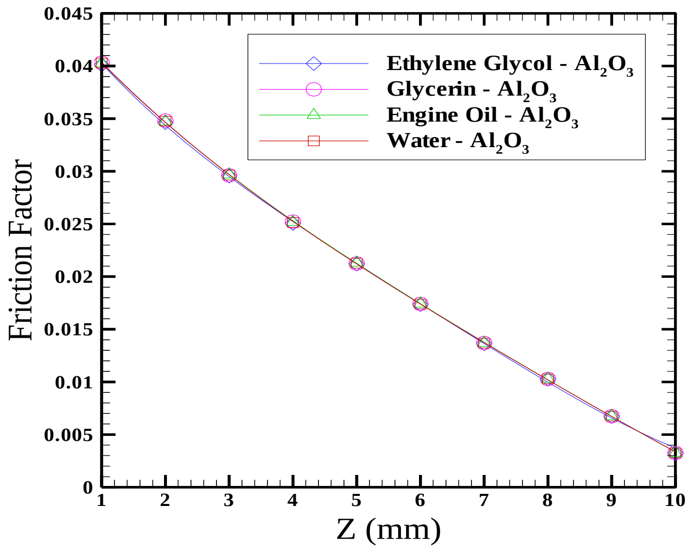

Fig. 7. Variation of friction factor of MCHS along the length of channel no. 14

3.5. Thermal Resistance

MCHS cooling performance using different types of nanofluids is assessed by exploring the results of thermal resistance (R_{th}) enhancement, as one may notice in Fig. 8. The thermal resistance equation can be defined as [21]:

$$R_{th} = \frac{T_{\max} - T_{inlet}}{q_w}, \tag{17}$$

where T_{max} is the maximum temperature in the heat sink and T_{inlet} is the inlet temperature. Pressure drop is another important parameter in MCHS performance, which is closely associated with pumping power coolant. To find out how the dimensional parameters affect the thermal performance, an optimal analysis should be used to compare the thermal resistance for different nanofluids.

The pumping power, $\overline{P}$, is determined as [22]:

$$\overline{P} = \dot{V}.\Delta p = N.u_{in}.A_c.\Delta p, \tag{18}$$

where $\dot{V}$ is the total volume flow rate, Δp is the pressure drop, N is the number of channels, u_{in} is the channel inlet velocity, A_c is the area of the cross-section of the channel, $A_{rhombus} = \frac{1}{2}P.Q$.

The MCHS cooling performance using nanofluids is compared based on examining the values of the thermal resistance enhancement versus the pumping power as presented in Fig. 8. The R_{th} and the areas of the cross-section for the pumping power are determined in Eqs. (17) and (18), respectively. The results show that water base fluids for Al_2O_3 have the lowest thermal resistance, which is equal to 0.051 ($K/kW/m^2$) and the lowest pumping power, due to the temperature difference decrease between inlet and maximum wall temperature. Finally, for removing the high feat flux from the cooling devices, rhombus microchannels heat sinks using nanofluids with pure water as base fluids can be proposed as next generation of base fluids.

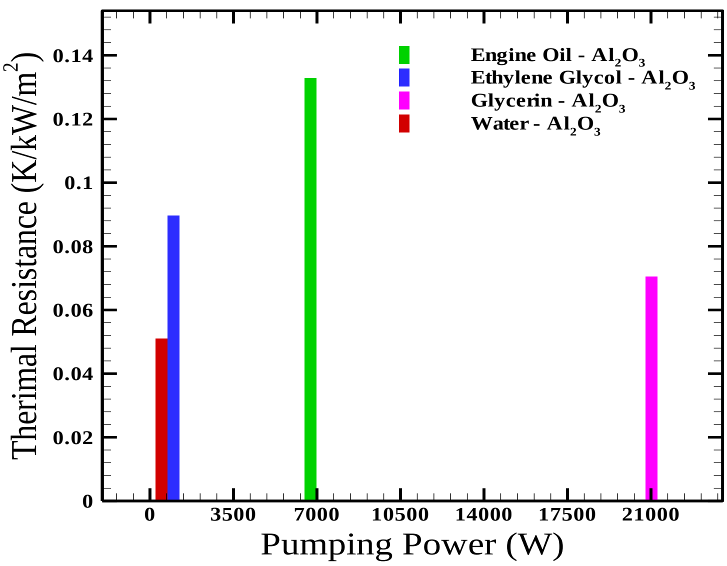

Fig. 8. Thermal resistance of MCHS as function of the pumping power

4. Conclusions

In this study, a 3D numerical model of laminar fluid flow and heat transfer characteristics in a rhombus microchannels heat sink are examined. The influences of using various types of base fluids mixed with Al_2O_3 nanoparticles on the MCHS performance were investigated. The most important findings of this study can be summarized as:

- Water-Al_2O_3 is preferred in cooled MCHS since water-Al_2O_3 has lower value of top wall temperature and higher value of heat transfer coefficient than other base fluids.
- The middle channel (no. 14) shows the highest heat transfer coefficient among all 25 channels.
- The base fluids friction factors have similar values for all types of base fluids.
- Water-Al_2O_3 as working fluids in rhombus shape cross-section MCHS has the lowest value of thermal resistance and pumping power.

R E F E R E N C E S

[1]. *H. Hadi Najafabadi, M. Keshavarz Moraveji*, “Three-dimensional CFD Modeling of Fluid Flow and Heat Transfer Characteristics of Al_2O_3/water Nanofluid in Microchannel Heat Sink with Eulerian-Eulerian Approach”, in Iranian Journal of Chemical Engineering, **vol. 13**, no. 4, Autumn 2016, IAChE

[2]. *C. Anbumeenakshi, M.R. Thansekhar*, “On the Effectiveness of a Nanofluid Cooled Microchannel Heat Sink Under Non-uniform Heating Condition”, in Applied Thermal Engineering, **vol. 113**, 2017, pp. 1437-1443

[3]. *R.N. Kumar, D.S. Kumar*, “*An experimental investigation on thermal performance of nanofluids in a minichannel heat sink*”, in Journal of Advances in chemistry **vol. 12**, ISSN 2321-807X, 2016

[4]. *Ayoub Abdollahi, H.A. Mohammed, Sh.M. Vanaki, A. Osia, M.R. Golbahar Haghighi*, “Fluid flow and heat transfer of nanofluids in microchannel heat sink with V-type inlet/outlet arrangement”, in Alexandria Engineering Journal, **vol. 56**, Issue 1, March 2017, pp. 161–170

[5]. *Cuneyt Uysal, Kamil Arslan, Huseyin Kurt*, “A Numerical Analysis of Fluid Flow and Heat Transfer Characteristics of ZnO-Ethylene Glycol Nanofluid in Rectangular Microchannels”, in Journal of Mechanical Engineering, **vol. 62**, no. 10, 2016, pp. 603-613

[6]. *Amit Agnihotri, Aashish Sharma*, “Three-Dimensional Heat Transfer Analysis of Microchannel Heat Sink Using Nanofluid”, in International Journal of Science, Technology & Management, **vol. 04**, Special Issue No. 01, March 2015, pp. 1199-1208

[7]. *A. Sivakumar, N. Alagumurthi, T. Senthilvelan*, “Experimental investigation of forced convective heat transfer performance in nanofluids of Al_2O_3/water and CuO/water in a serpentine shaped micro channel heat sink”, in Heat Mass Transfer, **vol. 52**, Iss. 7, July 2016, pp 1265–1274

[8]. *P. Rahim Mashaei1, S. M. Hosseinalipour, M. El Jawad Muslmani*, “The Impact of Nanoparticles on Forced Convection in a Serpentine Microchannel”, in Trans. Phenom. Nano Micro Scales, **vol. 2**, no. 2, Summer–Autumn 2014, pp. 86-99

[9]. *C.J. Ho, L.C. Wei, Z.W. Li*, “An experimental investigation of forced convective cooling performance of a microchannel heat sink with Al_2O_3/water nanofluid”, in Applied Thermal Engineering, **vol. 30**, 2010, pp. 96-103

[10]. *A.A. Alfaryjat, H.A. Mohammed, N.M. Adam, M.K.A. Ariffin, and M.I. Najafabadi*, "Influence of geometrical parameters of hexagonal, circular, and rhombus microchannel heat sinks on the thermohydraulic characteristics," in International Communications in Heat and Mass Transfer, **vol. 52** , 2014, pp. 121–131.

[11]. *S.V. Patankar*, Numerical Heat Transfer and Fluid Flow, Hemisphere, New York, 1980.

[12]. *H.K. Versteeg, W. Malalasekera*, An introduction to computational fluid dynamics: the finite volume method, John Wiley and Sons Inc, New York, 1995.

[13]. *B Ghasemi, S. M. Aminossadati*, “Brownian motion of nanoparticles in a triangular enclosure with natural convection”, in International Journal of Thermal Sciences, **vol. 49**, no. 6, 2010, pp. 931-940

[14]. *R. S. Vajjha, D. K. Das, D. P. Kulkarni*, “Development of new correlations for convective heat transfer and friction factor in turbulent regime for nanofluids”, in International Journal of Heat and Mass Transfer, **vol. 53**, no. 21, 2010, pp. 4607-4618

[15]. *R. S. Vajjha, D. K. Das*, “Experimental determination of thermal conductivity of three nanofluids and development of new correlations”, in International Journal of Heat and Mass Transfer, **vol. 52**, no. 21, 2009, pp. 4675-4682

[16]. *M. Corcione*, "Heat transfer features of buoyancy-driven nanofluids inside rectangular enclosures differentially heated at the sidewalls", in International Journal of Thermal Sciences, **vol. 49**, no. 9, 2010, pp. 1536-1546
[17]. *F. P., Incropera*, *D. P. De Witt*, Fundamentals of heat and mass transfer, John Wiley & Sons Inc., 1985.
[18]. *H.E. Ahmed, H.A. Mohammed, M.Z. Yusoff*, "An overview on heat transfer augmentation using vortex generators and nanofluids: Approaches and applications", in Renewable and Sustainable Energy Reviews, **vol. 16**, 2012, pp. 5951–5993
[19]. *X. Wang*, *X. Xu*, *S. U. S. Choi*, "Thermal conductivity of nanoparticle-fluid mixture", in Journal of Thermophysics and Heat Transfer, **vol. 13**, no. 4, 1999, pp. 474–480
[20]. *H. A. Mohammed, P. Gunnasegaran, N. H. Shuaib*, "Heat transfer in rectangular microchannels heat sink using nanofluids", in International Communications in Heat and Mass Transfer, **vol. 37**, 2010, pp. 1496-1503
[21]. *H.S. Kou*, *J.J. Lee*, *C.W. Chen*, "Optimum thermal performance of microchannel heat sink by adjusting channel width and height", Int. Commun. Heat Mass Transfer, **vol. 35**, 2008, pp. 577–582
[22]. *J. Li*, *G.P. Peterson*, "3-Dimensional numerical optimization of silicon-based high performance parallel microchannel heat sink with liquid flow", in International Journal of Heat and Mass Transfer, **vol. 50**, 2007, pp. 2895-2904